CSH PRESS
GENOME RESEARCH

Age-related epigenetic drift in the pathogenesis of MDS and AML

Shinji Maegawa, Sheryl Gough, Naoko Watanabe-Okochi, et al.

Genome Res. published online January 10, 2014
Access the most recent version at doi:10.1101/gr.157529.113

Title: Age-related epigenetic drift in the pathogenesis of MDS and AML

Authors: Shinji Maegawa,[1,2] Sheryl Gough,[3] Naoko Watanabe-Okochi,[4,5] Yue Lu,[2] Nianxiang Zhang,[6] Ryan J. Castoro,[2] Marcos R. H. Estecio,[2,7] Jaroslav Jelinek,[1,2] Shoudan Liang,[6] Toshio Kitamura,[4] Peter Aplan,[3] Jean-Pierre J. Issa[1,2]

Affiliations: [1]Fels Institute for Cancer Research and Molecular Biology, Temple University, Philadelphia, PA, United States of America, [2]Department of Leukemia, The University of Texas M. D. Anderson Cancer Center, Houston, TX, United States of America, [3]Genetics Branch, Center for Cancer Research, National Cancer Institute, National Institute of Health, Bethesda, MD, United States of America, [4]Division of Cellular Therapy, Advanced Clinical Research Center, The Institute of Medical Science, The University of Tokyo, Tokyo, Japan, [5]Department of Hematology & Oncology, Graduate School of Medicine, The University of Tokyo, Tokyo, Japan, [6]Department of Biostatistics and Computational Biology, The University of Texas M. D. Anderson Cancer Center, Houston, TX, United States of America, [7]Department of Molecular Carcinogenesis, The University of Texas M. D. Anderson Cancer Center, Houston, TX, United States of America

Corresponding author:

Shinji Maegawa, Fels Institute for Cancer Research and Molecular Biology, Temple University, Philadelphia, PA 19140. Phone: 215-707-3712; Fax: 215-707-4588; E-mail: shinji.maegawa@temple.edu

Running title: DNA methylation in MDS model mice

Keywords: DNA methylation, aging, MDS, AML

Manuscript type: Research

Abstract

The Myelodysplastic syndrome (MDS) is a clonal hematologic disorder that frequently evolves to acute myeloid leukemia (AML). Its pathogenesis remains unclear, but mutations in epigenetic modifiers are common and the disease often responds to DNA methylation inhibitors. We analyzed DNA methylation in the bone marrow and spleen in two mouse models of MDS/AML, the *NUP98-HOXD13* (*NHD13*) mouse and the *RUNX1* mutant mouse model. Methylation array analysis showed an average of 512/3445 (14.9%) genes hypermethylated in *NHD13* MDS and 331 (9.6%) genes hypermethylated in *RUNX1* MDS. 32% of genes in common between the two models (2/3 *NHD13* mice, and 2/3 *RUNX1* mice) were also hypermethylated in at least 2 out of 19 human MDS samples. Detailed analysis of 41 genes in mice showed progressively drift in DNA methylation from young to old normal bone marrow and spleen; to MDS, where we detected accelerated age-related methylation; and finally to AML, which markedly extends DNA methylation abnormalities. Most of these genes showed similar patterns in human MDS and AML. Repeat element hypomethylation was rare in MDS but marked the transition to AML in some cases. Our data show consistency in patterns of aberrant

DNA methylation in human and mouse MDS and suggest that epigenetically, MDS displays an accelerated aging phenotype.

Introduction

The Myelodysplastic syndrome (MDS) is a heterogeneous group of clonal stem-cell disorders characterized by ineffective hematopoiesis and susceptibility to leukemic transformation to acute myeloid leukemia (AML). A number of chromosomal abnormalities, including deletions, amplifications, inversions and translocations, have been identified in the malignant cells of patients with MDS, the most common of which are deletions of chromosomes 5q, 7q, and 20q(Haase et al. 2007). Mutations have been detected in genes that encode signal transduction proteins (*BRAF*, *CBL*, *GNAS*, *JAK2*, *KRAS*, *NRAS* and *PTPN11*), transcription factors and cofactors (*ETV6*, *NPM1*, *RUNX1* and *TP53*), cell cycle regulators (*CDKN2A* and *PTEN*)(Bejar et al. 2011), components of the RNA splicing machinery (*PRPF40B*, *SF1*, *SF3A1*, *SF3B1*, *SRSF2*, *U2AF1*, *U2AF2* and *ZRSR2*)(Yoshida et al. 2011), and most notably epigenetic modifiers (*ASXL1*, *DNMT3A*, *EZH2*, *IDH1/2* and *TET2*)(Shih et al. 2012). *TET2* is the most frequent gene abnormality in MDS(Kosmider et al. 2009; Langemeijer et al. 2009), and *DNMT3A* mutation is a very early genetic event in MDS(Walter et al. 2011). These mutations in epigenetic modifiers indicate that epigenetic changes contribute to MDS pathogenesis(Graubert and Walter 2011; Nikoloski et al. 2012).

DNA methylation is a well-established epigenetic mechanism that regulates gene transcription through modification of cytosines (usually but not always in the context of CpG dinucleotides(Xie et al. 2012; Varley et al. 2013)) and is frequently aberrant in human cancers. Hypermethylation at promoter CpG sites is common in human MDS, involving genes such as *CDH1*, *CDH13*, *CDKN2B*, *PDLIM4*, *PGR* and is a poor prognostic factor(Aggerholm et al. 2006; Issa 2010; Shen et al. 2010). Epigenetic therapy using hypomethylating agents such as azacitidine and decitabine has demonstrated clinical effectiveness in this disease. Both drugs are approved by the US Food and Drug Administration for the treatment of MDS(Kantarjian et al. 2006; Kantarjian et al. 2007; Bryan et al. 2010).

Recently, two mouse models for MDS and MDS/AML were established. In the first model a *NUP98-HOXD13* (*NHD13*) fusion transgene was inserted in the germline of C57BL/6 and FVB/N mice, using vav regulatory elements to direct expression specifically in hematopoietic tissues. *NHD13* transgenic mice faithfully recapitulate all the key features of MDS, including peripheral blood cytopenias, bone marrow dysplasia and increased apoptosis, and transformation to acute leukemia between 4 and 14 months of age(Lin et al. 2005; Slape et al. 2008). A second model uses bone marrow transplantation (BMT) of cells transduced with *RUNX1* mutants frequently found in patients with MDS and MDS/AML. A C-terminal truncation mutation of *RUNX1* caused by a frame-shift (S291fsX300, hereafter S291fs) induced pancytopenia associated with dysplasia in the erythroid lineage. A *RUNX1* point mutation in the Runt homology domain (RHD) (D171N) frequently induced hepatosplenomegaly and leukocytosis associated with marked myeloid dysplasia(Watanabe-Okochi et al. 2008). Cooperating genetic or epigenetic changes in these mouse models are incompletely understood.

Both models mimic aspects of human MDS/AML including an initial dyspoietic phase and progression to AML. The clinical course of the disease in these mice suggests that they provide a useful model for the human disease. We therefore studied DNA methylation of thousands of CpG sites by CpG island profiling in mouse spleen and bone marrow samples from normal and MDS model mice. We find a high rate of epigenetic deregulation in each model, with a significant number of shared events between the models and with human MDS. Epigenetically, MDS appears to be part of a continuum of changes that start in aging and culminate in AML.

Results

DNA methylation analysis in mouse models of MDS

To study the epigenetic evolution of normal cells to a malignant state in hematopoiesis, we used a total of 122 mouse samples. We summarize sample information such as genotypes and tissue types analyzed in Supplementary Table S1. We first examined three promoter CpG islands (*Cdh13*, *Esr1* and *Pgr*) which had previously been reported to be hypermethylated in human MDS(Shen et al. 2010). In all three, we found marked increases in methylation from normal to MDS to AML by using pyrosequencing analysis (Supplementary Figure S1 and Supplementary Table S2). Based on this candidate gene analyses, these MDS mouse models mimic aspects of human MDS methylation patterns and they were therefore studied in more detail.

We performed methylated CpG island amplification microarrays (MCAM) to study DNA methylation of thousands of genes(Estecio et al. 2007b; Yamamoto et al. 2012). Using normal spleen or normal bone marrow (transfected with empty vector) as age-matched control samples, we selected significantly altered autosomal genes based on a signal fold change greater than 2 (Figure 1A). We then performed unsupervised hierarchical cluster analysis of the data derived from six mice using variable probes that were changed at least in one out of six samples. The samples clustered into two major groups based on the models, as shown in Figure 1B. We studied three distinct *NHD13* mice at the MDS stage. Out of 3445 detectable genes, we found that 497, 490 and 548 were hypermethylated (average 512, 14.9%), and 190, 204 and 236 were hypomethylated (average 210, 6.1%) (Supplementary Table S3). Figure 1C shows (area-proportional) Venn diagrams indicating that 494 of 3445 detectable genes were hypermethylated in at least 2/3 *NHD13* MDS samples, while 199 genes were hypomethylated.

Next, we studied the *RUNX1* model. A total of 300, 270 and 665 genes were hypermethylated, and 125, 134 and 178 genes were hypomethylated in D171N (two individual mice) and S291fs, respectively (Supplementary Table S3). Figure 1D shows the overlapped genes among three individual mice in each model. A total of 147 hypermethylated genes and 28 hypomethylated genes overlapped in the *RUNX1* models. Finally, we examined gene overlap between the models. A total of 134 genes were hypermethylated and 37 genes hypomethylated in at least 2/3 *NHD13* and 2/3 *RUNX1* mice (Figure 1E). These included several cancer relevant genes such as *Gata5*, *Pax6*, *Sfrp1* and *Sox9*(Toyota et al. 1999; Suzuki et al. 2002; Akiyama et al. 2003; The Cancer Genome Atlas Network 2012). The names of the genes are shown in Supplementary Table S4.

Functional pathways affected

We examined the potential function of genes which showed common hypermethylation and hypomethylation in these MDS models. Transcriptional network and pathway analysis was performed on pair-wise comparisons between hypermethylated genes and detectable genes, and hypomethylated genes and detectable genes, respectively. Supplementary Table S5 shows the top five enriched categories for commonly hypermethylated genes in the mouse models. Hypermethylated genes showed significant enrichment for various developmental processes. The enriched molecular and cellular functions included cell development, signaling, growth and death. Enriched canonical pathways included Wnt/beta-catenin signaling. The list of hypomethylated genes was too short to analyze.

Age-related methylation drift in normal and malignant hematopoietic cells

To validate and quantitatively extend the array results, pyrosequencing analysis was used to study the methylation of 42 genes. Of these, 15 genes (*Asic2*, *Barhl2*, *Cdx2*, *Colec12*, *Crb3*, *Gng11*, *Hoxa2*, *Hoxc12*, *Hs3st2*, *Kcnma1*, *Ky*, *Lrig3*, *Syt10*, *Tlx3* and *Tmem229a*) were selected based solely on frequent hypermethylation detected by MCAM. 7 genes (*Bmi1*, *Elovl2*, *Fbn1*, *Hand2*, *Klf14*, *Pou4f2* and *Prdm5*) were selected based on prior publications showing age-related methylation(Maegawa et al. 2010; Hannum et al. 2013). Three genes (*Cdh13*, *Esr1* and *Pgr*) were selected from hypermethylated genes in human MDS as mentioned earlier(Shen et al. 2010). In addition, we selected 3 genes (*Espnl*, *Lims2* and *Olfr368*) based on MCAM data showing hypomethylation in MDS. Finally, 14 genes (*Cdh4*, *Cdkn1c*, *En2*, *Gata5*, *Gpr37*, *Grm7*, *Lrrtm1*, *Nptx2*, *Pax3*, *Pcdh10*, *Sox11*, *Tmeff2*, *Twist2* and *Wt1*) were selected based on MCAM data and also prior information on hypermethylation in mouse aging and/or human leukemias(Kay et al. 1997; Toyota et al. 2001; Shen et al. 2003; Rush et al. 2004; Raval et al. 2005; Ying et al.

2007; Kroeger et al. 2008; Bennett et al. 2009; Tong et al. 2010; Cosialls et al. 2012; Thathia et al. 2012). Out of all the selected genes, one (*Cdx2*) was a false positive (data not shown) and it was excluded from further analysis.

Quantitative analysis confirmed minimal (4.0-15.2%) methylation in normal bone marrow and spleen in 33 out of 38 genes (Figure 2A and Supplementary Figures S1 and S2). Five genes (*Esr1*, *Cdkn1c, Klf14, Hoxa2* and *Elovl2*) showed intermediate methylation percentages in normal tissues. *Esr1* corresponds to an exon 2 CpG island while the *Cdkn1c* and *Klf14* assay are in imprinted CpG islands(Bhogal et al. 2004; Parker-Katiraee et al. 2007; Maegawa et al. 2010). *Hoxa2* is about 50% methylated in normal and could be an imprinted gene(Luedi et al. 2007). The *Elovl2* assay is located outside of the CpG island (394bp upstream from TSS). We first studied age as a parameter that could influence DNA methylation in normal tissues and focused on the 38 genes hypermethylated in MDS/AML. We found linear hypermethylation with age (Supplementary Figure S3, Supplementary Table S6, and Figure 2B) for 31/38 genes in normal bone marrow (R>0.4 and p<0.05), 32/38 genes in normal spleen (R>0.4 and p<0.05) and 36/38 genes in either bone marrow (4), spleen (5) or both (27). Both tissues had a lower degree of methylation change than previously seen in mouse intestine(Maegawa et al. 2010). For bone marrow, there were only minor differences between the C57BL/6 strain (n=24) and the FVB/N strain (n=10). For spleen, we only studied C57BL/6 mice (n=34). Of note, all 15 genes selected solely because of frequent hypermethylation detected by MCAM showed age-related methylation drift. Thus, most genes frequently hypermethylated in mouse MDS also showed age-related methylation in normal hematopoietic tissues.

Next, we studied these 38 genes in MDS samples from spleen and bone marrow, and confirmed that all had higher methylation compared with normal samples (Figure 2A and Supplementary Figures S1 and S2, Supplementary Table S2). When we averaged all 38 genes, the methylation percentages were 30.4 and 28.8% in *RUNX1*-spleen and *NHD13*-bone marrow, respectively, compared to 16.8 and 11.8% in normal spleen and bone marrow (p<0.001 for both). There was also a progressive increase in hypermethylation in *NHD13*-AML samples transformed from MDS for all genes in spleen compared with the methylation percentage of normal and *NHD13*-MDS samples. We found 20.6% higher-average methylation for the 38 genes in AML-spleen (51.0%) compared to MDS-spleen (30.4%). Most of the genes followed an increasing methylation pattern in a phased manner from normal young (<1 y.o.), normal middle age (>1 y.o., <2 y.o.), normal old (>2 y.o.), to MDS and finally to AML samples (Figure 2A, Supplementary Figure S1 and S2, Supplementary Table S2). Hence, we found accelerated age-related hypermethylation in MDS progression, which is similar to what was previously reported in human colorectal cancer tumorigenesis(Toyota and Issa 1999; Issa et al. 2001).

In addition to hypermethylation, we analyzed hypomethylated genes by pyrosequencing analysis. We selected three genes (*Espnl*, *Lims2* and *Olfr368*) that showed hypomethylation in MDS based on MCAM analysis in mice (*Lims2* and *Olfr368*) or humans. *Espnl* was not detectable in mouse MCAM and was derived from human MCAM data (see below). All three were confirmed as hypomethylated in mouse MDS/AML (Supplementary Figure S2 and Supplementary Table S2) and all three were hypomethylated in aging spleen but not in aging bone marrow (Supplementary Figure S3 and Supplementary Table S6).

As a measure of CpG methylation specificity provided by the mutations of *RUNX1* and truncation of *NHD13*, we performed a two-dimensional hierarchical cluster analysis using the methylation % of the 38 genes studied by pyrosequencing. This analysis of DNA methylation divided all tissue samples into four major clusters (1 to 4) (Supplementary Figure S4). Cluster 1 contained 50/68 (74%) normal samples and 6/28 (21%) MDS samples. Cluster 2 and 3 contained mostly MDS while cluster 4 contained mostly AML. When we divided samples into each tissue type, hierarchical clustering also led to an almost perfect segregation of normal tissues depending on age (Supplementary Figure S5) and tumors based on their diagnostic criteria (Figure 3). In spleen, we found 3 major clusters; Cluster 1 includes all normal samples, Cluster 2 includes 53% of MDS and Cluster3 includes 83% of AML (Figure 3B). The ordering of samples by clustering analysis using the 38 genes closely reflected the number of methylated genes detected by MCAM (Figure 3), thus validating the array results.

Age-related drift and human MDS methylation

The candidate gene analysis suggested conservation between hypermethylated genes in human and mouse MDS. To study this more formally, we used MCAM analysis to study 19 human MDS patients (Supplementary Table S7). Out of 9645 detectable genes, we identified hypermethylated genes ranging from 205 to 1677 genes in all 19 patients (Supplementary Table S7). Unsupervised hierarchical clustering analysis identified 2 main clusters –one with high levels of DNA hypermethylation (designated

CIMP-positive), and one with low levels (designated CIMP-negative) (Figure 4A). The number of aberrantly hypermethylated genes was significantly higher in CIMP-positive cases (average 958 genes, 9.9%, compared to 403 genes, 4.2%, p<0.0001). CIMP-positive cases also had a higher ratio of the number of hypermethylated genes to the number of hypomethylated genes (Supplementary Figure S6A and Supplementary Table S7). We compared this CIMP classification to methylation levels of 9 genes (10 genomic regions), including *CDH1*, *CDH13*, *CDKN2B*, *ESR1*, *NPM2*, *OLIG2*, *OSCP1*, *PDLIM4* and *PGR*, previously studied by pyrosequencing analysis(Shen et al. 2010) in these cases. Most of the genes showed higher methylation in CIMP-positive cases (Supplementary Figure S6B). The averaged value of all 10 genomic regions was significantly higher in CIMP-positive patients compared to CIMP-negative patients (8.8±2.5% vs. 21.7±4.6%, p<0.0001) (Supplementary Figure S6B). We then looked for common hypermethylation events and found that 973 out of 9645 genes (10.1%) were hypermethylated in at least 3 out of 7 CIMP-positive patients compared with controls (Supplementary Table S8); these included genes involved in cell signaling, differentiation and cancer development (Supplementary Table S9). 294/9645 (3.0%) of genes showed MDS specific hypomethylation. In hypomethylated genes, enriched biological functions include cancer, developmental disorders (Supplementary Table S10).

We next cross-referenced methylated genes in human MDS and age-related genes reported in previous studies using whole blood. Out of 6294 detectable genes in our MCAM array, age-related hypermethylation was found in 573 genes (9.1%) by Horvath et al.(Horvath et al. 2012), 248 genes (3.9%) by Bell et al.(Bell et al. 2012) and 30 (0.35%) by Hannum et al.(Hannum et al. 2013). This wide range likely reflects different methods and criteria for selecting genes. Nevertheless, age-related methylated genes were significantly enriched among MDS methylated genes (2.1 fold, p<0.0001 for Horvath et al., 2.3 fold, p<0.0001 for Bell et al., 2.1 fold, p=0.047 for Hannum et al.). There were relatively few hypomethylated genes in all these data sets precluding a similar analysis. Thus, our data show a significant link between age-related methylation drift and MDS hypermethylation in humans.

Human – mouse MDS comparison

Because of a generally poor sequence conservation between mice and humans at promoter CpG islands(Antequera and Bird 1993; Matsuo et al. 1993), only 2344 genes could be compared directly (detectable on both human and mouse arrays). The accuracy of the comparison is also weakened by the fact that MCAM has limited precision (70-80% for random loci). We therefore focused on common methylation events. Of 346 genes hypermethylated in *NHD13* (2/3 mice) and detectable in the human arrays, 78 (23%) were also hypermethylated in human MDS (at least 2/19). When compared to the *RUNX1* models data, 77 out of 221 (35%) genes methylated in 2/3 *RUNX1* mice were also methylated in human MDS. Among 96 genes methylated in 2/3-*NHD13* and 2/3-*RUNX1* mice and detectable in human arrays, 31 (32%) were also methylated in human MDS (2/19) (Supplementary Table S11). In a search for driver events, we cross-referenced this list to the Cancer Gene Census (http://www.sanger.ac.uk/genetics/CGP/Census/) in COSMIC databases of cancer genes(Futreal et al. 2004) and identified several hits, including *CDH11*, *PAX3*, *TLX3* and

WT1. Thus there is partial conservation in MDS specific methylation between mice and humans.

Acceleration of age-related drift in human MDS/AML

To increase precision of the mouse – human comparison and to confirm human aging drift and acceleration of methylation from MDS to AML, we analyzed an unpublished data set of Digital Restriction Enzyme Analysis of Methylation (DREAM) in human cord blood (n=5), adult blood (n=13), MDS (n=20) and AML patients (n=94). DREAM has a high degree of quantitative accuracy thanks to deep sequencing(Challen et al. 2012; Jelinek et al. 2012). We focused on the 41 genes validated in the mouse model. Of these, 27/41 human homologous genes were detectable by DREAM at 118 SmaI sites (Supplementary Tables S12 and S13). We averaged the methylation status of SmaI sites (1-11 sites as listed in Supplementary Table S14) located in the promoter regions of each gene. Of the 27, 14 genes (51.9%) showed aging drift as hyper- or hypo-methylation with age (cord blood to adult blood), and 21 genes (77.8%) showed methylation acceleration from MDS to AML as shown in Figure 4B, Supplementary Figure S7 and Supplementary Table S14. 11 genes showed both features. Thus, the majority of genes that show validated epigenetic drift in mouse models of MDS/AML also show this in human MDS/AML.

Repetitive element methylation

In cancer, DNA hypomethylation typically occurs at repetitive sequences residing in satellite or pericentromeric regions, and can result in the reactivation of retrotransposons, leading to disruption of normal gene structure and function(Jones and Baylin 2002; Issa 2004; Estecio et al. 2007a). We studied global DNA methylation using pyrosequencing analysis of multiple DNA repetitive elements, such as long interspersed nuclear elements (LINE-1), major satellite repeats and short interspersed nuclear elements (SINE B1) in aging normal samples and MDS model samples. In spleen, we detected no significant change with age in LINE-1 or SINE B1 methylation, but major satellite methylation decreased from 74.3% to 68.4% in old mice (p=0.0006). This hypomethylation was not seen in bone marrow (Figure 5A).

In MDS mouse models, repetitive element methylation was generally unchanged or increased, compared to old mice. By contrast, the *NHD13*-AML samples showed significant hypomethylation in LINE-1 (35.5% to 31.7%, p=0.012) and SINE B1 (38.5% to 30.6%, p<0.0001), compared to normal spleen samples (Figure 5A). The methylation level of LINE-1 and SINE B1 correlated well (p<0.0001, R=0.63). We also found a significant but weaker association between the methylation level of LINE-1 and major satellite status (p=0.006, R=0.25) (Figure 5B).

Relation to polycomb targets and retrotransposon density

DNA hypermethylation in aging and cancer is more frequent among genes targeted by polycomb group (PcG) proteins in embryonic stem (ES) cells(Boyer et al. 2006; Lee et al. 2006; Ohm et al. 2007; Rauch et al. 2007; Schlesinger et al. 2007; Widschwendter et al. 2007; Maegawa et al. 2010; Teschendorff et al. 2010) and among genes with few retrotransposons around their promoter(Estecio et al. 2010). To study this for MDS, we first evaluated whether PcG targets in ES cells are enriched in the group of genes showing MDS specific methylation in mouse and human, by using databases of PcG occupancy in mouse ES cells(Boyer et al. 2006; Lee et al. 2006). There was 1.5 and 4.7 fold enrichment in SUZ12 targets on average in *NHD13* and *RUNX1* MDS model specific hypermethylation compared with non-targets among detectable genes ($p<0.0001$, Chi-square test). Similarly, EED, RNF2 and PHC1 targets are enriched among hypermethylated genes in each MDS model (Supplementary Table S15). There was no PcG target enrichment among hypomethylated genes (Supplementary Table S15). Similarly, PcG targets in human ES cells are also prone to MDS specific hypermethylation compared with all detectable genes. SUZ12 and EED targets are associated with 4.2 and 4.3 fold increase, respectively ($p<0.0001$, Chi-square test) (Supplementary Table S15).

We next looked at the presence of SINE B1 elements around gene promoters(Estecio et al. 2010). We found that genomic regions hypermethylated in *NHD13* and *RUNX1* model were less frequently associated with the presence of SINE B1 elements than a set of control genes that have promoter CpG islands (Supplementary Figure S8). Similar to other human cancers previously reported(Estecio et al. 2010), we also found the depleted presence of SINE B1 around gene promoters in human MDS (Supplementary Figure S8).

Discussion

Here, we report on epigenetic analysis of mouse models of MDS and show extensive DNA methylation abnormalities that overlap with those seen in human MDS.

We further demonstrate that methylation changes arise as a function of age in normal hematopoiesis and are accelerated in MDS and at the transition from MDS to AML. We analyzed two different MDS mouse models mimicking human MDS and found similar patterns in both, with appreciable overlap with the aberrant DNA methylation phenotype in human MDS. Thus, these oncogene driven models parallel the human disease both genetically and epigenetically, and are worth studying further from a therapeutic perspective, for example to optimize established treatments and discover new drugs (e.g. epigenetic drugs).

We focused on DNA methylation status because aberrant DNA methylation is believed to be a hallmark of preneoplastic and neoplastic conditions(Jones and Baylin 2002; Jones and Baylin 2007). Hypermethylation of promoters rich in CpG sites is associated with gene silencing which can be epigenetically inherited across cell divisions(Jones and Baylin 2002; Jones and Baylin 2007), and methylation provides a memory of the silent gene expression state(Raynal et al. 2012). Hypermethylation-induced silencing of genes was previously described in human MDS for individual genes and limited genome-wide studies(Boultwood and Wainscoat 2007; Issa 2010). Here, using methylation arrays, we show abnormal promoter methylation in about one-tenth of the genes analyzed in human MDS as well as in mouse MDS models compared with control cells. Our results are qualitatively similar to a previous array-based DNA methylation profiling study of 807 genes chosen on the basis of their importance to cancer development and progression(Jiang et al. 2009). One limitation of these studies is the use of unfractionated bone marrow or blood derived mononuclear cells. Contamination with non-affected cells can reduce the sensitivity of the analyses, and it is theoretically possible that different methylation patterns can be seen in different MDS cellular fractions. However, we have previously shown that, for aberrant promoter hypermethylation, similar results can been in human MDS derived from marrow or blood(Shen et al. 2010), and we have also shown that promoter DNA methylation is identical in AML progenitor and differentiated cells(Yamazaki et al. 2013). These previous results and the clonal nature of DNA methylation propagation suggest that the changes observed here are occurring in the MDS stem cell. In addition to promoter hypermethylation and hypomethylation, we also found hypomethylation as measured by repetitive element methylation but this appeared to be a progression event in these models, as it is in other human malignancies(Chalitchagorn et al. 2004; Estecio et al. 2007a).

In this study, we did not sort undifferentiated leukemic cells. It therefore remains possible that genes we identified could be linked with cell differentiation. Previously, Bock et al. had reported that methylation changes during differentiation occur mostly in non-promoter regions(Bock et al. 2012). In that study, 162, 160 and 157 genes increased methylation from multipotent progenitor 1 (Flt3 negative) to T helper cell (CD4 positive), cytotoxic T-cell (CD8 positive) and B-cell respectively. Out of these, none was detected as specifically hypermethylated in mouse MDS among 19, 22 and 24 detectable genes in the MCAM assay. In the same study, 247 genes showed increase methylation during hematopoietic differentiation from hematopoietic stem cells into progenitor cells and the average levels of increases were 10-17% of methylation. Among these, 24 were detectable by MCAM and only two (*Rarb* and *Rtkn*) were hypermethylated in mouse

MDS. Thus, most of the genes (132/134 genes) detected as hypermethylated in mouse MDS were unrelated to cell differentiation.

Quantitative analysis of methylation using pyrosequencing allowed us to unequivocally show that most of the leukemia associated changes actually arise in aging hematopoietic cells, be it spleen or bone marrow derived (in mice). The data confirm that epigenetic drift (so called because both hyper and hypomethylation can be seen with age depending on the gene studied) is a major cause of neoplasm-associated changes in DNA methylation in both solid(Toyota and Issa 1999; Ahuja and Issa 2000) and liquid tumors and are consistent with a model whereby age-related drift creates epigenetic variation. In turn, we speculate that variation provides the necessary ingredient for natural selection to promote the growth of pre-neoplastic (and eventually neoplastic) lesions. In spontaneous leukemogenesis, epigenetic drift likely precedes critical genetic changes but the mouse models show that the order can be reversed, with selection for epigenetic changes being part of the secondary changes that lead to disease evolution in *NHD13* and *RUNX1* models. Interestingly, MDS has intermediate levels of methylation drift compared to AML and, epigenetically, cells studies at the MDS stage appear to have an accelerated aging phenotype, as previously seen in chronic inflammatory conditions(Hsieh et al. 1998; Issa et al. 2001; Sato et al. 2002; Ushijima and Okochi-Takada 2005; Hahn et al. 2008; Chiba et al. 2012). The factors that lead to epigenetic drift in the first place remain unclear, though we show here that both polycomb occupancy in embryonic stem cells and depletion of retrotransposons around transcription sites are accelerating factors, as previously seen in other tissues(Widschwendter et al. 2007; Estecio et al. 2010).

The methylation data in the 19 human MDS patients studied by MCAM was heterogeneous, with a subset of cases having very high levels of promoter-CpG island methylation, suggestive of CIMP. Some of these same patients were previously studied for a panel of 9 genes (10 genomic regions) and the results were concordant with the current study, thus confirming the extensive nature of CIMP in MDS. The causes of this phenotype are unknown. It was previously suggested that *TET2* or *IDH1/2* mutations can cause CIMP in AML(Figueroa et al. 2010), but we have not found an association between *TET2* mutations and CpG island methylation in CMML(Yamazaki et al. 2012) and this was not seen in TCGA data sets either(The Cancer Genome Atlas Resarch Network 2013). It has been previously suggested that methylation heterogeneity might be related to heterogeneity in genetic backgrounds and/or differences in exposures to carcinogens or diet. However, even in the MDS mouse models with a uniform genetic background and exposures, we also found methylation-prone and methylation-resistant MDS by pyrosequencing analysis. Thus, the mechanisms responsible for producing methylation variation must involve stochastic events that, however, remain unknown.

The methylated genes we identified here have roles in multiple cellular functions, including cell-signaling, regulation of development, differentiation and tumorigenesis. This observation agrees with other reports that many fundamental pathways related to tumor pathogenesis are inactivated by methylation(Baylin and Ohm 2006). Some of them overlap with the genes listed as cancer genes related to leukemias and lymphomas(Futreal et al. 2004). However, it is important to keep in mind that only a minority of the genes aberrantly methylated in cancer are driver events, and identification of these remains a difficult proposition. For genetic events frequency points to drivers but for DNA methylation, frequency may point to intrinsic gene susceptibility rather than function/selection(Estecio et al. 2010). Indeed, many of the known tumor-suppressors hypermethylated in cancer and leukemias have methylation frequencies of 10-30% only in target malignancies (e.g. *CDKN2B* in AML, *CDKN2A* in colon cancer and melanoma, *VHL* in renal cancer etc.)(Herman et al. 1994; Gonzalgo et al. 1997; Baylin and Herman 2000; Rashid et al. 2001; Raj et al. 2007; Jonsson et al. 2010). It is possible that shared lesions in mouse and human leukemogenesis may point to driver genes, and we identified some potential examples such as *PAX3*, *TLX3*, *ALK* and *GATA2*. The functional significance of hypermethylation of these genes needs to be determined in future studies.

Methods

Tissue samples

We studied a total of 122 mouse samples including normal tissues, *NHD13* mice and *RUNX1* mice (Supplementary Table S1). We also studied 19 samples of human MDS whose characteristics were previously reported(Shen et al. 2010) (Supplementary Table S7).

MCAM

MCAM was performed as described previously(Maegawa et al. 2010). We used genomic DNA form normal whole bone marrow to test the malignant bone marrow tissues derived from model mice as a control. Previously, we found minimal differences in DNA methylation of CpG islands between CD34+ bone marrow cells and mononuclear cells, and CD34+ bone marrow cells and unsorted peripheral white blood cells in human MCAM experiments, and we found no differences between stem cells and progenitor cells(Yamazaki et al. 2013), suggesting that the chosen control was appropriate for MCAM analysis. Mouse and human promoter arrays were purchased from Agilent Technologies (Agilent, Santa Clara, CA). After washing, arrays were scanned on an Agilent scanner and analyzed using Agilent Feature Extraction software at the M. D. Anderson Microarray Core Facility. We analyzed array data using a database that includes probe sequences, length of SmaI fragments, chromosomal regions and localization of repetitive elements. The ratios of hybridization intensities were adjusted by using Lowess normalization.

Pathway analyses

Functional class scoring analysis was performed on hyper or hypo- methylated genes with each genotype by using the Ingenuity pathway analysis software. We analyzed biological processes, molecular functions and cellular components that were relatively enriched by the gene lists of interest using the detectable genes as reference set.

Bisulfite pyrosequencing for promoter and global DNA methylation analysis

Bisulfite treatment using the EpiTect Bisulfite Kit was performed according to the manufacturer's instructions (Qiagen). We used a quantitative bisulfite pyrosequencing method for all DNA methylation analyses as reported previously(Maegawa et al. 2010). Primer sequences and PCR conditions for bisulfite pyrosequencing assays are listed in Supplementary Table S16. Primer sequences and conditions used for human promoter methylation determination are described in previous publication(Shen et al. 2010). For each assay, we used fully methylated DNA prepared by treating genomic DNA with SssI methylase (New England Biolabs, Beverly, MA) as a positive control.

Statistics

All correlation was calculated using Spearman's correlation analysis. Calculations were done using GraphPad Prism 4.0 (GraphPad Software Inc., San Diego, CA). All p-values are two-sided. Hierarchical clustering for MCAM result was performed in Partek Software. Euclidean distance dissimilarities and Ward's method were used to cluster both genes and samples. For clustering analysis in pyrosequencing result, we used ArrayTrack Software available at http://edkb.fda.gov/webstart/arraytrack/.

Data access

The microarray data from this study have been submitted to the GEO (http://www.ncbi.nlm.nih.gov/geo/) under accession no. GSE46067.

Acknowledgments

This work was supported by National Institutes of Health grants CA100632, CA158112 and CA108631 and by a grant from the Ellison Medical Foundation. JPI is an American Cancer Society Clinical Research professor supported by a generous gift from the F. M. Kirby Foundation.

Figure legends

Fig. 1. MCAM analysis in mouse MDS models. (A) R-I plot of the probes with FDR at 5% and fold change >2 for MCAM. An R-I plot displays the log2(R/G) ratio for each element on the array as a function of the log10(R*G) product intensities and can reveal systematic intensity-dependent effects in the measured log2 (ratio) values. The red and blue spots indicate probes hypermethylated and hypomethylated in diseased samples, respectively. (B) Hierarchical clustering analysis of mouse MCAM. Heat-map analysis showing the MCAM results in 6 model mice. Red, yellow and blue correspond to hypermethylated, non-changed and hypomethylated loci, respectively. For clarity we excluded probes that were unchanged in all samples. (C) Venn diagram of individual differences of hyper- and hypomethylated genes in *NHD13* mice analyzed by MCAM. Each circle represents one individual. (D) Venn diagram of mutational differences of hyper- and hypomethylated genes in *RUNX1* mice analyzed by MCAM. Each circle represents one individual. (E) Venn diagram of hyper- and hypomethylated genes overlapped between *NHD13* and *RUNX1* mice analyzed by MCAM. Each circle means each genotype.

Fig. 2. DNA methylation profiles by bisulfite pyrosequencing analysis. (A) DNA methylation analysis in MDS mice. The percentages of methylated cytosines in the samples as obtained from pyrosequencing analysis. Each dot corresponds to one animal. We show here data on *Grm7*, *Hand2*, *Hoxc12*, *Klf14* and *Sox11*. The other 33 hypermethylated genes are shown in Supplementary Figure S1 and Supplementary Figure S2. The averaged data was derived from methylation data of 38 genes prone to

hypermethylation. The bar in the graphs represents the median. (B) Methylation profiles of hypermethylated genes with age in mouse bone marrow and spleen. Association of the averaged percentages of methylated cytosines in the samples as obtained from pyrosequencing (y-axis) with age (x-axis) for significant genes.

Fig. 3. Hierarchical clustering analysis of methylation markers in mouse. (A) Hierarchical clustering analysis in bone marrow. Green to red cells indicated the range of methylation percentage from 0 to 95.3. The color codes for mouse strain, tissues, age and diagnosis are listed left side. Orange arrowheads indicate samples for MCAM with number of methylated genes by MCAM. (B) Hierarchical clustering analysis in spleen.

Fig. 4. DNA methylation analyses in humans. (A) Hierarchical clustering analysis of human MCAM. Heat-map analysis showing the MCAM results in 19 MDS patients. Red, yellow and blue correspond to hypermethylated, non-changed and hypomethylated loci, respectively. All probes that were unchanged in all samples were excluded from the analysis. The bar graph on the left shows the methylation % of LINE-1 by pyrosequencing analysis. Red-colored boxes on the right side represent CIMP-positive case defined by MCAM assay. (B) DNA methylation profiles by DREAM analysis in human cord blood, adult blood, MDS and AML patients. The percentages of methylated cytosines in the samples as obtained from DREAM analysis. Each dot corresponds to one individual. We show here data on *HOXC12*, *SOX11* and *ESPNL*. The averaged data was derived from methylation data of 26 hypermethylated genes listed in Supplementary Table S14. The bar in the graphs represents the median.

Fig. 5. Methylation analysis of repetitive elements in mouse. (A) methylation profiles of LINE-1, SINE B1 and major satellite DNA by pyrosequencing analysis. (B) Association of the methylation percentages between LINE-1 (y-axis), SINE B1 (x-axis) and major satellite DNA (x-axis) in the all samples. Color codes are on the right. The Spearman test was used to determine correlations, with significance set at $p < 0.05$. R represents a measure of the linear relationship between two variables, and varies from -1 to +1.

Supplementary information

Supplementary Fig. S1.

DNA methylation analysis of candidate genes in MDS mice. These 3 genes were chosen because their human homologous genes were reported as hypermethylated in human MDS. Shown are the percentages of methylated cytosines in the samples as obtained from pyrosequencing analysis. Each dot corresponds to one animal. The bar in the graphs represents the median.

Supplementary Fig. S2.

DNA methylation analysis in MDS mice. Shown are the percentages of methylated cytosines in the samples as obtained from pyrosequencing analysis. Shown are all of the genes analyzed except the 5 genes in Figure 2A and the 3 genes in Supplementary Figure S1. Gene selection is described in the text. Each dot corresponds to one animal. The bar in the graphs represents the median.

Supplementary Fig. S3.

Methylation profiles of hyper- or hypomethylated genes with age in mouse bone marrow and spleen. Association of the percentages of methylated cytosines in the samples as obtained from pyrosequencing (y-axis) with age (x-axis) for 41 genes. Red dots and line, and blue dots and line indicate spleen and bone marrow, respectively.

Supplementary Fig. S4.

Hierarchical clustering analysis of methylation markers in all mouse samples studied. Color codes are on the left bottom. The bar graph on the top shows the methylation % of LINE-1 by pyrosequencing analysis.

Supplementary Fig. S5.

Hierarchical clustering analysis of methylation markers in mouse. (A) Hierarchical clustering analysis in normal bone marrow. Green to red cells indicated the range of methylation percentage from 0 to 57.3. The color code for age is listed on the bottom. (B) Hierarchical clustering analysis in normal spleen.

Supplementary Fig. S6.

DNA methylation analysis in human MDS patients. (A) Number of hyper- and hypomethylated genes detected by MCAM assay. All 19 patients were categorized into CIMP-positive or CIMP-negative based on MCAM data. (B) Differences of methylation % of 9 genes (10 genomic regions) between CIMP-positive and CIMP-negative patients. Averaged levels are shown on the right side. The bar in the graphs represents the median.

Supplementary Fig. S7.

DNA methylation analysis in human cord blood, adult blood, MDS and AML patients. Shown are the percentages of methylated cytosines in the samples as obtained from DREAM analysis. Shown are all of the genes analyzed except the 3 genes in Figure 4B. Each dot corresponds to one individual. The bar in the graphs represents the median.

Supplementary Fig. S8.

Appearance ratio of SINE B1 elements in human MDS and *RUNX1* MDS model. X-axis (1 to 10) means distance from transcription start site (kb). Minus indicates upstream of transcripts. Red line indicates hypermethylated genes by MCAM. Blue and black lines indicate hypomethylated genes and genes which has CpG island.

Supplementary Table S1.

Mice samples analyzed.

Supplementary Table S2.

Summary of p-values obtained from t-tests comparing methylation percentages detected by pyrosequencing analysis.

Supplementary Table S3.

Summary of MCAM data in mouse models.

Supplementary Table S4.

Hyper- and hypomethylated genes in MDS models analyzed by MCAM.

Supplementary Table S5.

Significant terms in Ingenuity pathway analysis in mouse MDS models.

Supplementary Table S6.

Summary of r-values and p-values from spearman correlation between methylation percentages and age in mouse bone marrow and spleen.

Supplementary Table S7.

Summary of MCAM data in human MDS patients.

Supplementary Table S8.

Hyper- and hypomethylated genes in human MDS patients analyzed by MCAM.

Supplementary Table S9.

Significant terms in Ingenuity pathway analysis in human MDS patients for hypermethylated genes.

Supplementary Table S10.

Significant terms in Ingenuity pathway analysis in human MDS patients for hypomethylated genes.

Supplementary Table S11.

Overlapped genes between mouse models and human MDS patients.

Supplementary Table S12.

Raw data detected by DREAM in human samples.

Supplementary Table S13.

Normalized methylation values detected by DREAM in human samples.

Supplementary Table S14.

Summary of p-values obtained from t-tests comparing methylation percentages detected by DREAM analysis.

Supplementary Table S15.

Methylation change by polycomb status in MDS models and human MDS patients.

Supplementary Table S16.

Mouse primer sequences and PCR conditions for bisulfite pyrosequencing analysis.

References

Aggerholm A, Holm MS, Guldberg P, Olesen LH, Hokland P. 2006. Promoter hypermethylation of p15INK4B, HIC1, CDH1, and ER is frequent in myelodysplastic syndrome and predicts poor prognosis in early-stage patients. *European journal of haematology* **76**(1): 23-32.

Ahuja N, Issa JP. 2000. Aging, methylation and cancer. *Histology and histopathology* **15**(3): 835-842.

Akiyama Y, Watkins N, Suzuki H, Jair KW, van Engeland M, Esteller M, Sakai H, Ren CY, Yuasa Y, Herman JG et al. 2003. GATA-4 and GATA-5 transcription factor genes and potential downstream antitumor target genes are epigenetically silenced in colorectal and gastric cancer. *Molecular and cellular biology* **23**(23): 8429-8439.

Antequera F, Bird A. 1993. Number of CpG islands and genes in human and mouse. *Proceedings of the National Academy of Sciences of the United States of America* **90**(24): 11995-11999.

Baylin SB, Herman JG. 2000. DNA hypermethylation in tumorigenesis: epigenetics joins genetics. *Trends in genetics : TIG* **16**(4): 168-174.

Baylin SB, Ohm JE. 2006. Epigenetic gene silencing in cancer - a mechanism for early oncogenic pathway addiction? *Nature reviews Cancer* **6**(2): 107-116.

Bejar R, Stevenson K, Abdel-Wahab O, Galili N, Nilsson B, Garcia-Manero G, Kantarjian H, Raza A, Levine RL, Neuberg D et al. 2011. Clinical effect of point mutations in myelodysplastic syndromes. *The New England journal of medicine* **364**(26): 2496-2506.

Bell JT, Tsai PC, Yang TP, Pidsley R, Nisbet J, Glass D, Mangino M, Zhai G, Zhang F, Valdes A et al. 2012. Epigenome-wide scans identify differentially methylated regions for age and age-related phenotypes in a healthy ageing population. *PLoS genetics* **8**(4): e1002629.

Bennett LB, Schnabel JL, Kelchen JM, Taylor KH, Guo J, Arthur GL, Papageorgio CN, Shi H, Caldwell CW. 2009. DNA hypermethylation accompanied by transcriptional repression in follicular lymphoma. *Genes, chromosomes & cancer* **48**(9): 828-841.

Bhogal B, Arnaudo A, Dymkowski A, Best A, Davis TL. 2004. Methylation at mouse Cdkn1c is acquired during postimplantation development and functions to maintain imprinted expression. *Genomics* **84**(6): 961-970.

Bock C, Beerman I, Lien WH, Smith ZD, Gu H, Boyle P, Gnirke A, Fuchs E, Rossi DJ, Meissner A. 2012. DNA methylation dynamics during in vivo differentiation of blood and skin stem cells. *Molecular cell* **47**(4): 633-647.

Boultwood J, Wainscoat JS. 2007. Gene silencing by DNA methylation in haematological malignancies. *British journal of haematology* **138**(1): 3-11.

Boyer LA, Plath K, Zeitlinger J, Brambrink T, Medeiros LA, Lee TI, Levine SS, Wernig M, Tajonar A, Ray MK et al. 2006. Polycomb complexes repress developmental regulators in murine embryonic stem cells. *Nature* **441**(7091): 349-353.

Bryan J, Jabbour E, Prescott H, Garcia-Manero G, Issa JP, Kantarjian H. 2010. Current and future management options for myelodysplastic syndromes. *Drugs* **70**(11): 1381-1394.

The Cancer Genome Atlas Network. 2012. Comprehensive molecular characterization of human colon and rectal cancer. *Nature* **487**(7407): 330-337.

The Cancer Genome Atlas Research Network. 2013. Genomic and epigenomic landscapes of adult de novo acute myeloid leukemia. *The New England journal of medicine* **368**(22): 2059-2074.

Chalitchagorn K, Shuangshoti S, Hourpai N, Kongruttanachok N, Tangkijvanich P, Thong-ngam D, Voravud N, Sriuranpong V, Mutirangura A. 2004. Distinctive pattern of LINE-1 methylation level in normal tissues and the association with carcinogenesis. *Oncogene* **23**(54): 8841-8846.

Challen GA, Sun D, Jeong M, Luo M, Jelinek J, Berg JS, Bock C, Vasanthakumar A, Gu H, Xi Y et al. 2012. Dnmt3a is essential for hematopoietic stem cell differentiation. *Nature genetics* **44**(1): 23-31.

Chiba T, Marusawa H, Ushijima T. 2012. Inflammation-associated cancer development in digestive organs: mechanisms and roles for genetic and epigenetic modulation. *Gastroenterology* **143**(3): 550-563.

Cosialls AM, Santidrian AF, Coll-Mulet L, Iglesias-Serret D, Gonzalez-Girones DM, Perez-Perarnau A, Rubio-Patino C, Gonzalez-Barca E, Alonso E, Pons G et al. 2012. Epigenetic profile in chronic lymphocytic leukemia using methylation-specific multiplex ligation-dependent probe amplification. *Epigenomics* **4**(5): 491-501.

Estecio MR, Gallegos J, Vallot C, Castoro RJ, Chung W, Maegawa S, Oki Y, Kondo Y, Jelinek J, Shen L et al. 2010. Genome architecture marked by retrotransposons modulates predisposition to DNA methylation in cancer. *Genome research* **20**(10): 1369-1382.

Estecio MR, Gharibyan V, Shen L, Ibrahim AE, Doshi K, He R, Jelinek J, Yang AS, Yan PS, Huang TH et al. 2007a. LINE-1 hypomethylation in cancer is highly variable and inversely correlated with microsatellite instability. *PloS one* **2**(5): e399.

Estecio MR, Yan PS, Ibrahim AE, Tellez CS, Shen L, Huang TH, Issa JP. 2007b. High-throughput methylation profiling by MCA coupled to CpG island microarray. *Genome research* **17**(10): 1529-1536.

Figueroa ME, Abdel-Wahab O, Lu C, Ward PS, Patel J, Shih A, Li Y, Bhagwat N, Vasanthakumar A, Fernandez HF et al. 2010. Leukemic IDH1 and IDH2 mutations result in a hypermethylation phenotype, disrupt TET2 function, and impair hematopoietic differentiation. *Cancer cell* **18**(6): 553-567.

Futreal PA, Coin L, Marshall M, Down T, Hubbard T, Wooster R, Rahman N, Stratton MR. 2004. A census of human cancer genes. *Nature reviews Cancer* **4**(3): 177-183.

Gonzalgo ML, Bender CM, You EH, Glendening JM, Flores JF, Walker GJ, Hayward NK, Jones PA, Fountain JW. 1997. Low frequency of p16/CDKN2A methylation in sporadic melanoma: comparative approaches for methylation analysis of primary tumors. *Cancer research* **57**(23): 5336-5347.

Graubert T, Walter MJ. 2011. Genetics of myelodysplastic syndromes: new insights. *Hematology / the Education Program of the American Society of Hematology American Society of Hematology Education Program* **2011**: 543-549.

Haase D, Germing U, Schanz J, Pfeilstocker M, Nosslinger T, Hildebrandt B, Kundgen A, Lubbert M, Kunzmann R, Giagounidis AA et al. 2007. New insights into the prognostic impact of the karyotype in MDS and correlation with subtypes: evidence from a core dataset of 2124 patients. *Blood* **110**(13): 4385-4395.

Hahn MA, Hahn T, Lee DH, Esworthy RS, Kim BW, Riggs AD, Chu FF, Pfeifer GP. 2008. Methylation of polycomb target genes in intestinal cancer is mediated by inflammation. *Cancer research* **68**(24): 10280-10289.

Hannum G, Guinney J, Zhao L, Zhang L, Hughes G, Sadda S, Klotzle B, Bibikova M, Fan JB, Gao Y et al. 2013. Genome-wide methylation profiles reveal quantitative views of human aging rates. *Molecular cell* **49**(2): 359-367.

Herman JG, Latif F, Weng Y, Lerman MI, Zbar B, Liu S, Samid D, Duan DS, Gnarra JR, Linehan WM et al. 1994. Silencing of the VHL tumor-suppressor gene by DNA methylation in renal carcinoma. *Proceedings of the National Academy of Sciences of the United States of America* **91**(21): 9700-9704.

Horvath S, Zhang Y, Langfelder P, Kahn RS, Boks MP, van Eijk K, van den Berg LH, Ophoff RA. 2012. Aging effects on DNA methylation modules in human brain and blood tissue. *Genome biology* **13**(10): R97.

Hsieh CJ, Klump B, Holzmann K, Borchard F, Gregor M, Porschen R. 1998. Hypermethylation of the p16INK4a promoter in colectomy specimens of patients with long-standing and extensive ulcerative colitis. *Cancer research* **58**(17): 3942-3945.

Issa JP. 2004. CpG island methylator phenotype in cancer. *Nature reviews Cancer* **4**(12): 988-993.

-. 2010. Epigenetic changes in the myelodysplastic syndrome. *Hematology/oncology clinics of North America* **24**(2): 317-330.

Issa JP, Ahuja N, Toyota M, Bronner MP, Brentnall TA. 2001. Accelerated age-related CpG island methylation in ulcerative colitis. *Cancer research* **61**(9): 3573-3577.

Jelinek J, Liang S, Lu Y, He R, Ramagli LS, Shpall EJ, Estecio MR, Issa JP. 2012. Conserved DNA methylation patterns in healthy blood cells and extensive changes in leukemia measured by a new quantitative technique. *Epigenetics : official journal of the DNA Methylation Society* **7**(12): 1368-1378.

Jiang Y, Dunbar A, Gondek LP, Mohan S, Rataul M, O'Keefe C, Sekeres M, Saunthararajah Y, Maciejewski JP. 2009. Aberrant DNA methylation is a dominant mechanism in MDS progression to AML. *Blood* **113**(6): 1315-1325.

Jones PA, Baylin SB. 2002. The fundamental role of epigenetic events in cancer. *Nature reviews Genetics* **3**(6): 415-428.

-. 2007. The epigenomics of cancer. *Cell* **128**(4): 683-692.

Jonsson A, Tuominen R, Grafstrom E, Hansson J, Egyhazi S. 2010. High frequency of p16(INK4A) promoter methylation in NRAS-mutated cutaneous melanoma. *The Journal of investigative dermatology* **130**(12): 2809-2817.

Kantarjian H, Issa JP, Rosenfeld CS, Bennett JM, Albitar M, DiPersio J, Klimek V, Slack J, de Castro C, Ravandi F et al. 2006. Decitabine improves patient outcomes in myelodysplastic syndromes: results of a phase III randomized study. *Cancer* **106**(8): 1794-1803.

Kantarjian H, Oki Y, Garcia-Manero G, Huang X, O'Brien S, Cortes J, Faderl S, Bueso-Ramos C, Ravandi F, Estrov Z et al. 2007. Results of a randomized study of 3 schedules of low-dose decitabine in higher-risk myelodysplastic syndrome and chronic myelomonocytic leukemia. *Blood* **109**(1): 52-57.

Kay PH, Spagnolo DV, Taylor J, Ziman M. 1997. DNA methylation and developmental genes in lymphomagenesis--more questions than answers? *Leukemia & lymphoma* **24**(3-4): 211-220.

Kosmider O, Gelsi-Boyer V, Cheok M, Grabar S, Della-Valle V, Picard F, Viguie F, Quesnel B, Beyne-Rauzy O, Solary E et al. 2009. TET2 mutation is an independent favorable prognostic factor in myelodysplastic syndromes (MDSs). *Blood* **114**(15): 3285-3291.

Kroeger H, Jelinek J, Estecio MR, He R, Kondo K, Chung W, Zhang L, Shen L, Kantarjian HM, Bueso-Ramos CE et al. 2008. Aberrant CpG island methylation in acute myeloid leukemia is accentuated at relapse. *Blood* **112**(4): 1366-1373.

Langemeijer SM, Kuiper RP, Berends M, Knops R, Aslanyan MG, Massop M, Stevens-Linders E, van Hoogen P, van Kessel AG, Raymakers RA et al. 2009. Acquired mutations in TET2 are common in myelodysplastic syndromes. *Nature genetics* **41**(7): 838-842.

Lee TI, Jenner RG, Boyer LA, Guenther MG, Levine SS, Kumar RM, Chevalier B, Johnstone SE, Cole MF, Isono K et al. 2006. Control of developmental regulators by Polycomb in human embryonic stem cells. *Cell* **125**(2): 301-313.

Lin YW, Slape C, Zhang Z, Aplan PD. 2005. NUP98-HOXD13 transgenic mice develop a highly penetrant, severe myelodysplastic syndrome that progresses to acute leukemia. *Blood* **106**(1): 287-295.

Luedi PP, Dietrich FS, Weidman JR, Bosko JM, Jirtle RL, Hartemink AJ. 2007. Computational and experimental identification of novel human imprinted genes. *Genome research* **17**(12): 1723-1730.

Maegawa S, Hinkal G, Kim HS, Shen L, Zhang L, Zhang J, Zhang N, Liang S, Donehower LA, Issa JP. 2010. Widespread and tissue specific age-related DNA methylation changes in mice. *Genome research* **20**(3): 332-340.

Matsuo K, Clay O, Takahashi T, Silke J, Schaffner W. 1993. Evidence for erosion of mouse CpG islands during mammalian evolution. *Somatic cell and molecular genetics* **19**(6): 543-555.

Nikoloski G, van der Reijden BA, Jansen JH. 2012. Mutations in epigenetic regulators in myelodysplastic syndromes. *International journal of hematology* **95**(1): 8-16.

Ohm JE, McGarvey KM, Yu X, Cheng L, Schuebel KE, Cope L, Mohammad HP, Chen W, Daniel VC, Yu W et al. 2007. A stem cell-like chromatin pattern may predispose tumor suppressor genes to DNA hypermethylation and heritable silencing. *Nature genetics* **39**(2): 237-242.

Parker-Katiraee L, Carson AR, Yamada T, Arnaud P, Feil R, Abu-Amero SN, Moore GE, Kaneda M, Perry GH, Stone AC et al. 2007. Identification of the imprinted KLF14 transcription factor undergoing human-specific accelerated evolution. *PLoS genetics* **3**(5): e65.

Raj K, John A, Ho A, Chronis C, Khan S, Samuel J, Pomplun S, Thomas NS, Mufti GJ. 2007. CDKN2B methylation status and isolated chromosome 7 abnormalities predict responses to treatment with 5-azacytidine. *Leukemia : official journal of the Leukemia Society of America, Leukemia Research Fund, UK* **21**(9): 1937-1944.

Rashid A, Shen L, Morris JS, Issa JP, Hamilton SR. 2001. CpG island methylation in colorectal adenomas. *The American journal of pathology* **159**(3): 1129-1135.

Rauch T, Wang Z, Zhang X, Zhong X, Wu X, Lau SK, Kernstine KH, Riggs AD, Pfeifer GP. 2007. Homeobox gene methylation in lung cancer studied by genome-wide analysis with a microarray-based methylated CpG island recovery assay. *Proceedings of the National Academy of Sciences of the United States of America* **104**(13): 5527-5532.

Raval A, Lucas DM, Matkovic JJ, Bennett KL, Liyanarachchi S, Young DC, Rassenti L, Kipps TJ, Grever MR, Byrd JC et al. 2005. TWIST2 demonstrates differential methylation in immunoglobulin variable heavy chain mutated and unmutated chronic lymphocytic leukemia. *Journal of clinical oncology : official journal of the American Society of Clinical Oncology* **23**(17): 3877-3885.

Raynal NJ, Si J, Taby RF, Gharibyan V, Ahmed S, Jelinek J, Estecio MR, Issa JP. 2012. DNA methylation does not stably lock gene expression but instead serves as a molecular mark for gene silencing memory. *Cancer research* **72**(5): 1170-1181.

Rush LJ, Raval A, Funchain P, Johnson AJ, Smith L, Lucas DM, Bembea M, Liu TH, Heerema NA, Rassenti L et al. 2004. Epigenetic profiling in chronic lymphocytic leukemia reveals novel methylation targets. *Cancer research* **64**(7): 2424-2433.

Sato F, Harpaz N, Shibata D, Xu Y, Yin J, Mori Y, Zou TT, Wang S, Desai K, Leytin A et al. 2002. Hypermethylation of the p14(ARF) gene in ulcerative colitis-associated colorectal carcinogenesis. *Cancer research* **62**(4): 1148-1151.

Schlesinger Y, Straussman R, Keshet I, Farkash S, Hecht M, Zimmerman J, Eden E, Yakhini Z, Ben-Shushan E, Reubinoff BE et al. 2007. Polycomb-mediated methylation on Lys27 of histone H3 pre-marks genes for de novo methylation in cancer. *Nature genetics* **39**(2): 232-236.

Shen L, Kantarjian H, Guo Y, Lin E, Shan J, Huang X, Berry D, Ahmed S, Zhu W, Pierce S et al. 2010. DNA methylation predicts survival and response to therapy in patients with myelodysplastic syndromes. *Journal of clinical oncology : official journal of the American Society of Clinical Oncology* **28**(4): 605-613.

Shen L, Toyota M, Kondo Y, Obata T, Daniel S, Pierce S, Imai K, Kantarjian HM, Issa JP, Garcia-Manero G. 2003. Aberrant DNA methylation of p57KIP2 identifies a cell-cycle regulatory pathway with prognostic impact in adult acute lymphocytic leukemia. *Blood* **101**(10): 4131-4136.

Shih AH, Abdel-Wahab O, Patel JP, Levine RL. 2012. The role of mutations in epigenetic regulators in myeloid malignancies. *Nature reviews Cancer* **12**(9): 599-612.

Slape C, Liu LY, Beachy S, Aplan PD. 2008. Leukemic transformation in mice expressing a NUP98-HOXD13 transgene is accompanied by spontaneous mutations in Nras, Kras, and Cbl. *Blood* **112**(5): 2017-2019.

Suzuki H, Gabrielson E, Chen W, Anbazhagan R, van Engeland M, Weijenberg MP, Herman JG, Baylin SB. 2002. A genomic screen for genes upregulated by demethylation and histone deacetylase inhibition in human colorectal cancer. *Nature genetics* **31**(2): 141-149.

Teschendorff AE, Menon U, Gentry-Maharaj A, Ramus SJ, Weisenberger DJ, Shen H, Campan M, Noushmehr H, Bell CG, Maxwell AP et al. 2010. Age-dependent DNA methylation of genes that are suppressed in stem cells is a hallmark of cancer. *Genome research* **20**(4): 440-446.

Thathia SH, Ferguson S, Gautrey HE, van Otterdijk SD, Hili M, Rand V, Moorman AV, Meyer S, Brown R, Strathdee G. 2012. Epigenetic inactivation of TWIST2 in acute lymphoblastic leukemia modulates proliferation, cell survival and chemosensitivity. *Haematologica* **97**(3): 371-378.

Tong WG, Wierda WG, Lin E, Kuang SQ, Bekele BN, Estrov Z, Wei Y, Yang H, Keating MJ, Garcia-Manero G. 2010. Genome-wide DNA methylation profiling of chronic lymphocytic leukemia allows identification of epigenetically repressed molecular pathways with clinical impact. *Epigenetics : official journal of the DNA Methylation Society* **5**(6): 499-508.

Toyota M, Ho C, Ahuja N, Jair KW, Li Q, Ohe-Toyota M, Baylin SB, Issa JP. 1999. Identification of differentially methylated sequences in colorectal cancer by methylated CpG island amplification. *Cancer research* **59**(10): 2307-2312.

Toyota M, Issa JP. 1999. CpG island methylator phenotypes in aging and cancer. *Seminars in cancer biology* **9**(5): 349-357.

Toyota M, Kopecky KJ, Toyota MO, Jair KW, Willman CL, Issa JP. 2001. Methylation profiling in acute myeloid leukemia. *Blood* **97**(9): 2823-2829.

Ushijima T, Okochi-Takada E. 2005. Aberrant methylations in cancer cells: where do they come from? *Cancer science* **96**(4): 206-211.

Varley KE, Gertz J, Bowling KM, Parker SL, Reddy TE, Pauli-Behn F, Cross MK, Williams BA, Stamatoyannopoulos JA, Crawford GE et al. 2013. Dynamic DNA methylation across diverse human cell lines and tissues. *Genome research* **23**(3): 555-567.

Walter MJ, Ding L, Shen D, Shao J, Grillot M, McLellan M, Fulton R, Schmidt H, Kalicki-Veizer J, O'Laughlin M et al. 2011. Recurrent DNMT3A mutations in patients with myelodysplastic syndromes. *Leukemia : official journal of the Leukemia Society of America, Leukemia Research Fund, UK* **25**(7): 1153-1158.

Watanabe-Okochi N, Kitaura J, Ono R, Harada H, Harada Y, Komeno Y, Nakajima H, Nosaka T, Inaba T, Kitamura T. 2008. AML1 mutations induced MDS and MDS/AML in a mouse BMT model. *Blood* **111**(8): 4297-4308.

Widschwendter M, Fiegl H, Egle D, Mueller-Holzner E, Spizzo G, Marth C, Weisenberger DJ, Campan M, Young J, Jacobs I et al. 2007. Epigenetic stem cell signature in cancer. *Nature genetics* **39**(2): 157-158.

Xie W, Barr CL, Kim A, Yue F, Lee AY, Eubanks J, Dempster EL, Ren B. 2012. Base-resolution analyses of sequence and parent-of-origin dependent DNA methylation in the mouse genome. *Cell* **148**(4): 816-831.

Yamamoto E, Suzuki H, Yamano HO, Maruyama R, Nojima M, Kamimae S, Sawada T, Ashida M, Yoshikawa K, Kimura T et al. 2012. Molecular dissection of premalignant colorectal lesions reveals early onset of the CpG island methylator phenotype. *The American journal of pathology* **181**(5): 1847-1861.

Yamazaki J, Estecio MR, Lu Y, Long H, Malouf GG, Graber D, Huo Y, Ramagli L, Liang S, Kornblau SM et al. 2013. The epigenome of AML stem and progenitor cells. *Epigenetics : official journal of the DNA Methylation Society* **8**(1): 92-104.

Yamazaki J, Taby R, Vasanthakumar A, Macrae T, Ostler KR, Shen L, Kantarjian HM, Estecio MR, Jelinek J, Godley LA et al. 2012. Effects of TET2 mutations on DNA methylation in chronic myelomonocytic leukemia. *Epigenetics : official journal of the DNA Methylation Society* **7**(2): 201-207.

Ying J, Gao Z, Li H, Srivastava G, Murray PG, Goh HK, Lim CY, Wang Y, Marafioti T, Mason DY et al. 2007. Frequent epigenetic silencing of protocadherin 10 by methylation in multiple haematologic malignancies. *British journal of haematology* **136**(6): 829-832.

Yoshida K, Sanada M, Shiraishi Y, Nowak D, Nagata Y, Yamamoto R, Sato Y, Sato-Otsubo A, Kon A, Nagasaki M et al. 2011. Frequent pathway mutations of splicing machinery in myelodysplasia. *Nature* **478**(7367): 64-69.

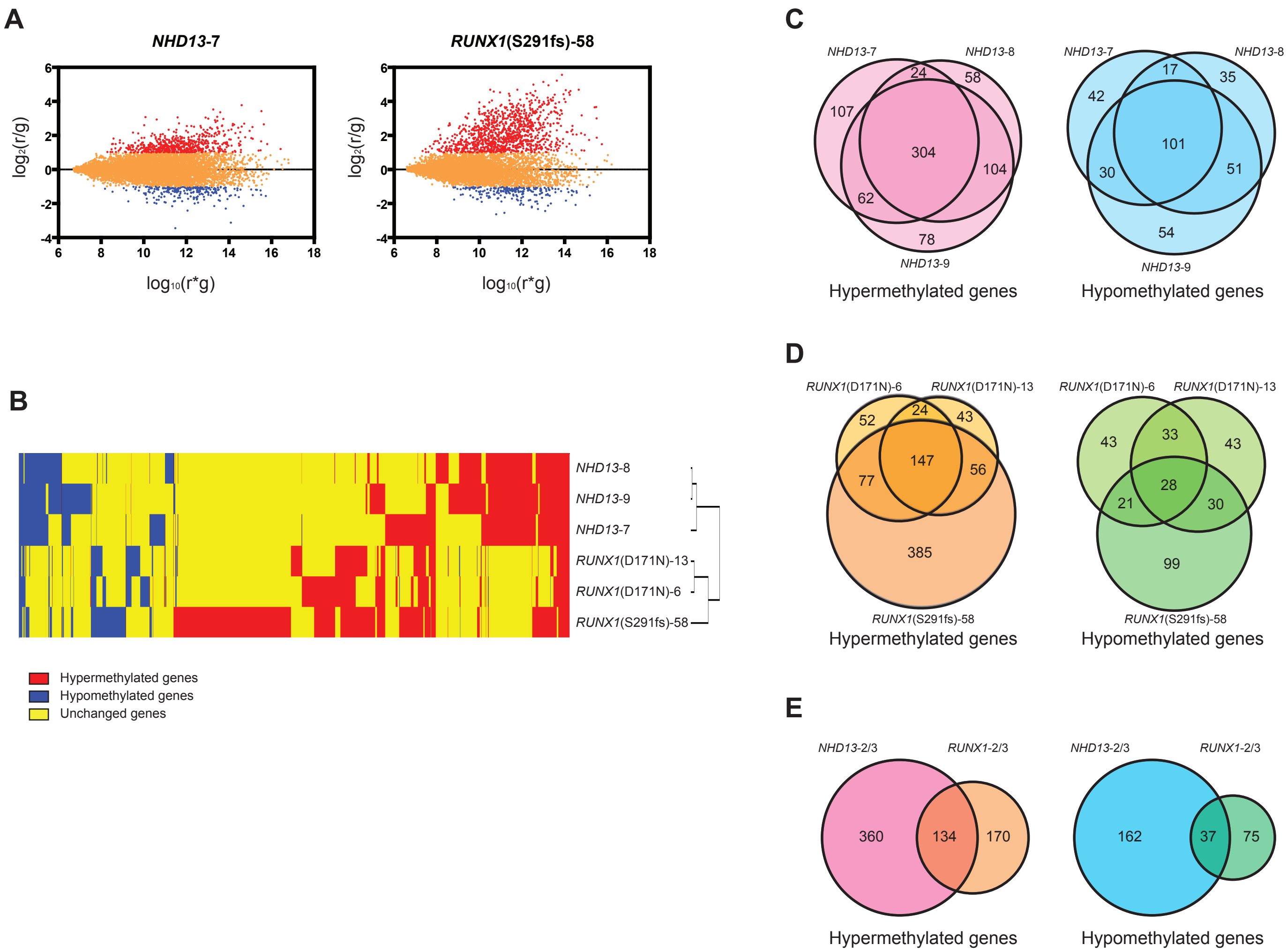
A
NHD13-7
RUNX1(S291fs)-58
log2(r/g)
log10(r*g)
B
NHD13-8
NHD13-9
NHD13-7
RUNX1(D171N)-13
RUNX1(D171N)-6
RUNX1(S291fs)-58
Hypermethylated genes
Hypomethylated genes
Unchanged genes
C
NHD13-7
NHD13-8
NHD13-9
107
24
58
304
104
62
78
Hypermethylated genes
42
17
35
101
30
51
54
Hypomethylated genes
D
RUNX1(D171N)-6
RUNX1(D171N)-13
RUNX1(S291fs)-58
52
24
43
147
77
56
385
Hypermethylated genes
43
33
43
28
21
30
99
Hypomethylated genes
E
NHD13-2/3
RUNX1-2/3
360
134
170
Hypermethylated genes
162
37
75
Hypomethylated genes

Figure 1

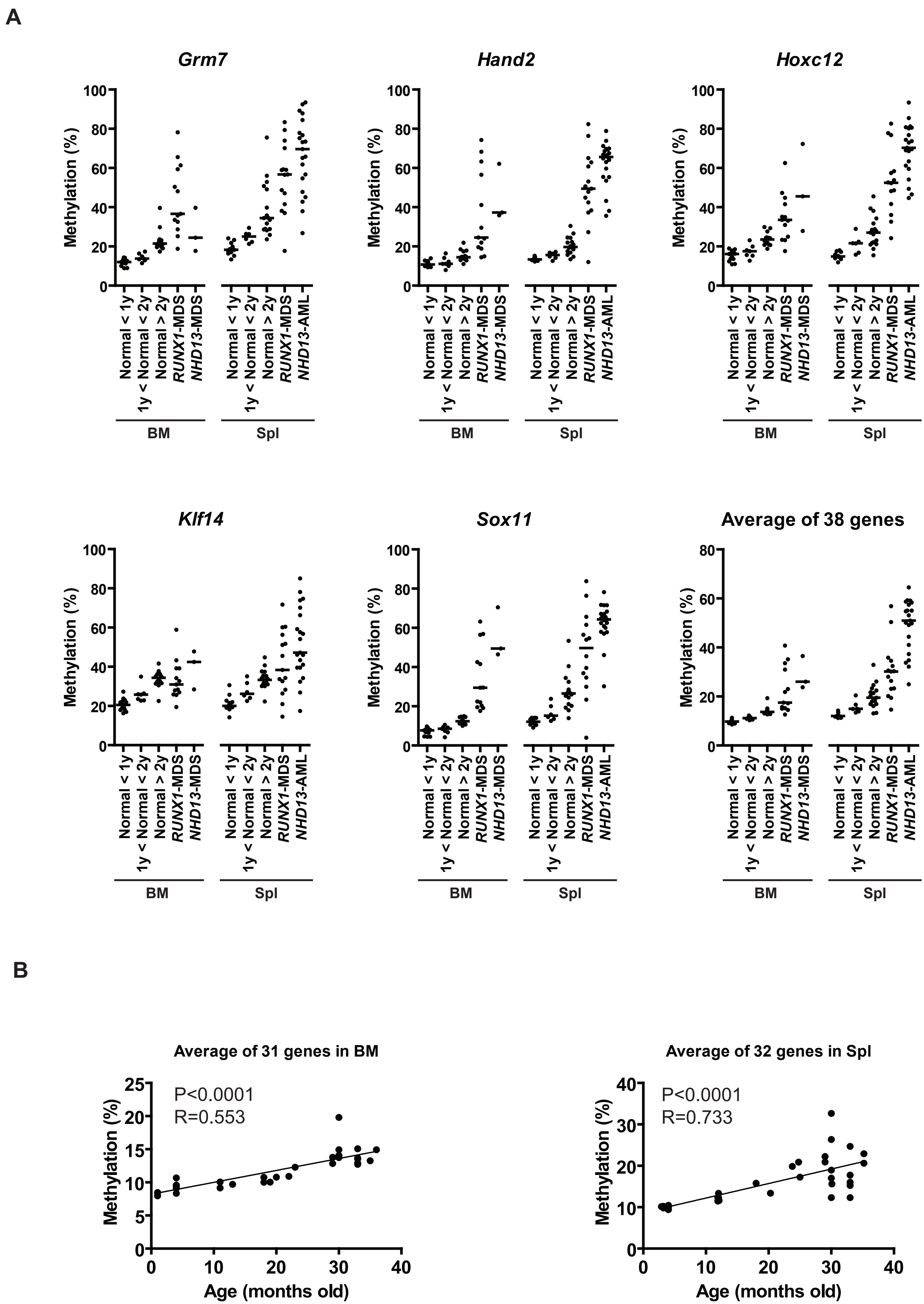
A
Grm7
Hand2
Hoxc12
Klf14
Sox11
Average of 38 genes
Methylation (%)
Normal < 1y
1y < Normal < 2y
Normal > 2y
RUNX1-MDS
NHD13-MDS
NHD13-AML
BM
Spl
B
Average of 31 genes in BM
P<0.0001
R=0.553
Average of 32 genes in Spl
P<0.0001
R=0.733
Methylation (%)
Age (months old)

Figure 2

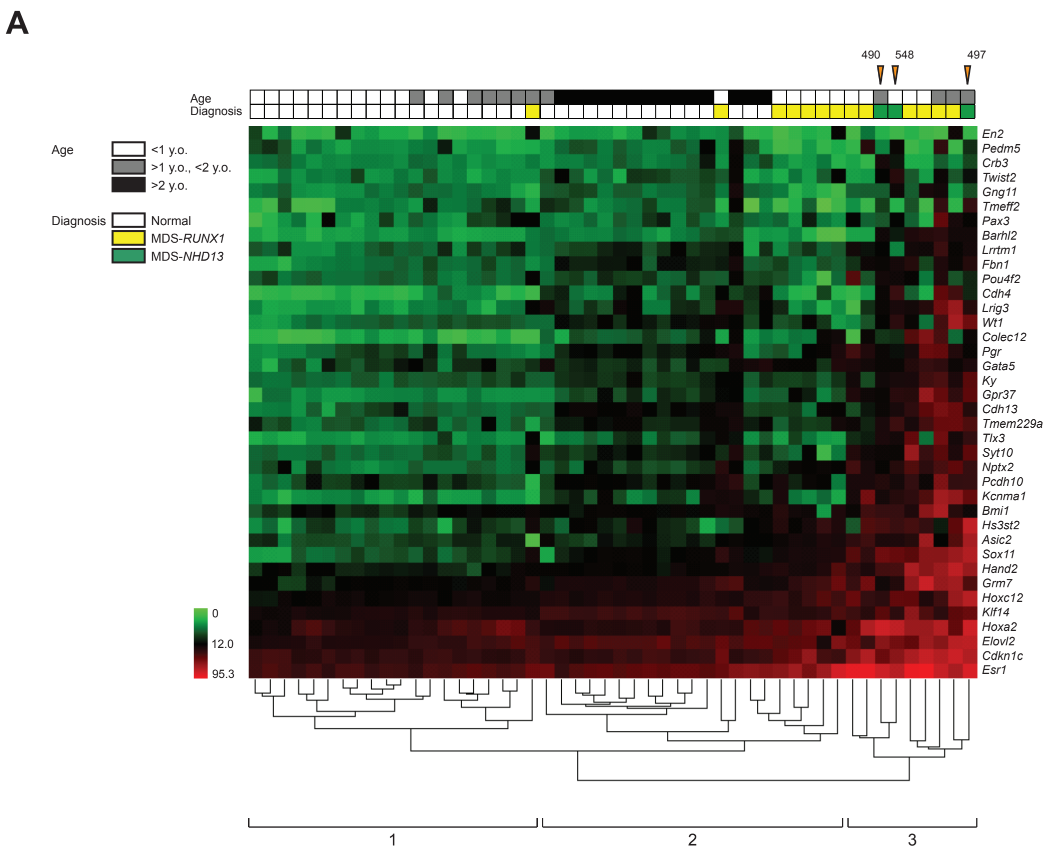
A
490
548
497
Age
Diagnosis
Age
<1 y.o.
>1 y.o., <2 y.o.
>2 y.o.
Diagnosis
Normal
MDS-RUNX1
MDS-NHD13
En2
Pedm5
Crb3
Twist2
Gng11
Tmeff2
Pax3
Barhl2
Lrrtm1
Fbn1
Pou4f2
Cdh4
Lrig3
Wt1
Colec12
Pgr
Gata5
Ky
Gpr37
Cdh13
Tmem229a
Tlx3
Syt10
Nptx2
Pcdh10
Kcnma1
Bmi1
Hs3st2
Asic2
Sox11
Hand2
Grm7
Hoxc12
Klf14
Hoxa2
Elovl2
Cdkn1c
Esr1
0
12.0
95.3
1
2
3

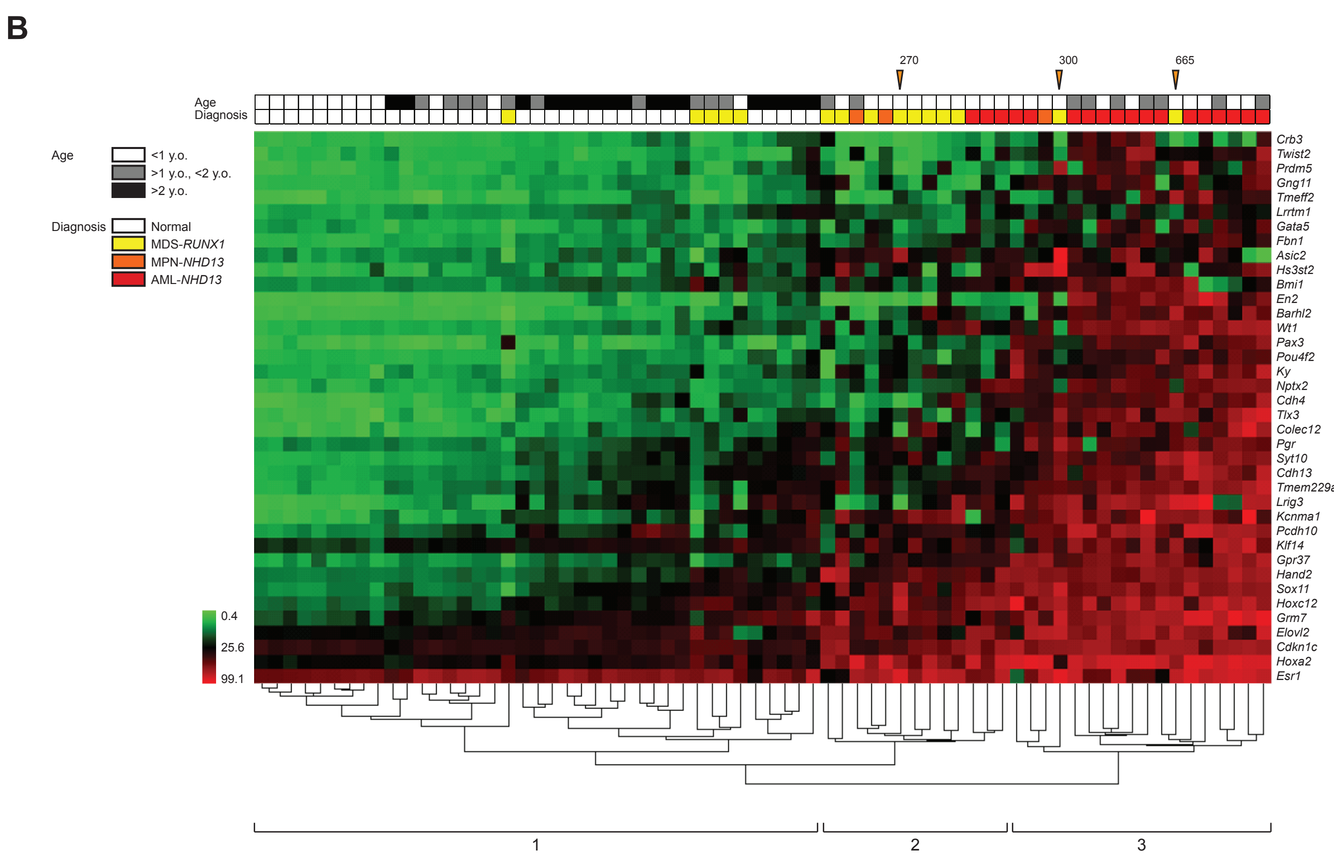
B
270
300
665
Age
Diagnosis
Age
<1 y.o.
>1 y.o., <2 y.o.
>2 y.o.
Diagnosis
Normal
MDS-RUNX1
MPN-NHD13
AML-NHD13
Crb3
Twist2
Prdm5
Gng11
Tmeff2
Lrrtm1
Gata5
Fbn1
Asic2
Hs3st2
Bmi1
En2
Barhl2
Wt1
Pax3
Pou4f2
Ky
Nptx2
Cdh4
Tlx3
Colec12
Pgr
Syt10
Cdh13
Tmem229a
Lrig3
Kcnma1
Pcdh10
Klf14
Gpr37
Hand2
Sox11
Hoxc12
Grm7
Elovl2
Cdkn1c
Hoxa2
Esr1
0.4
25.6
99.1
1
2
3

Figure 3

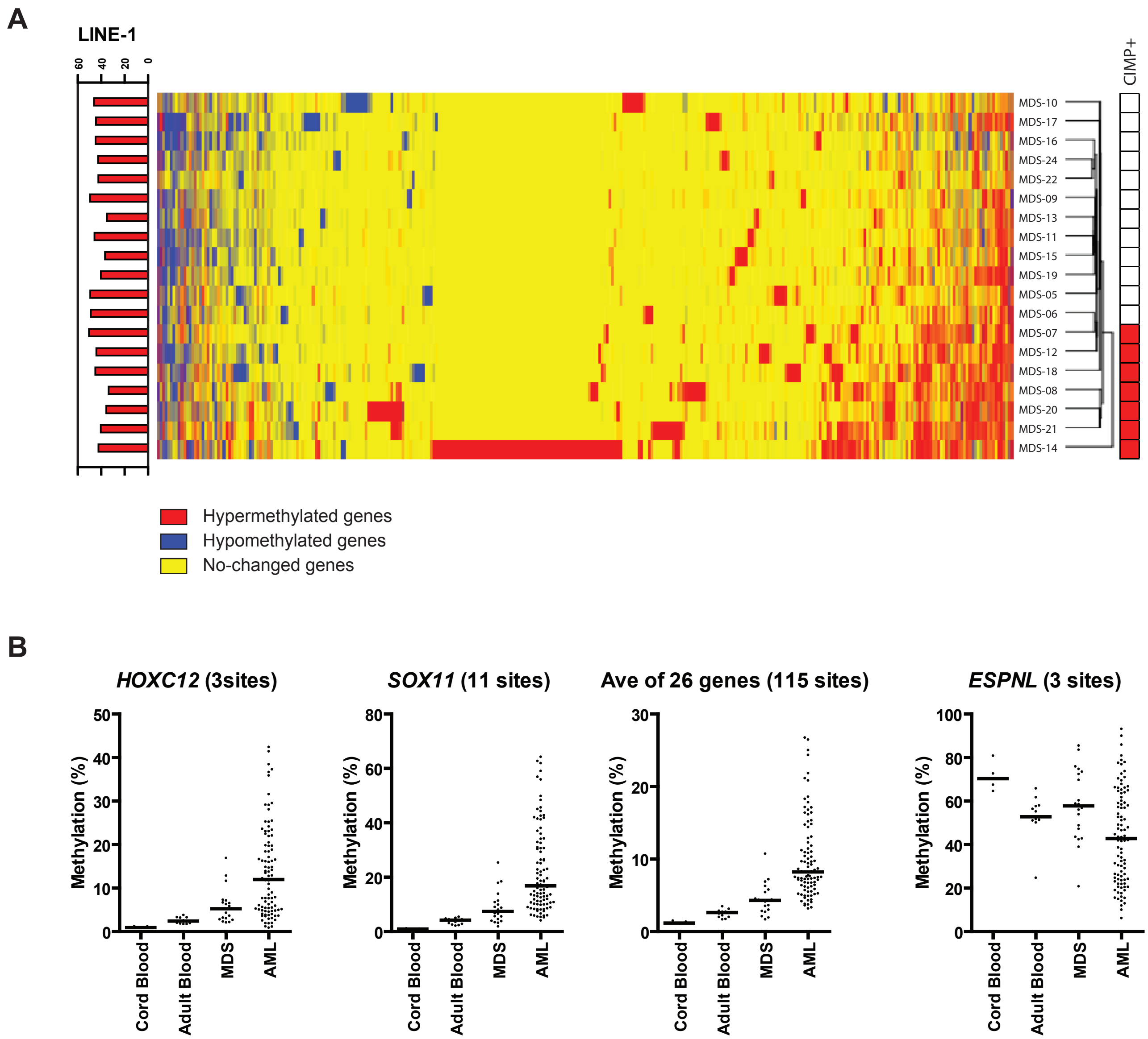
A
LINE-1
60
40
20
0
CIMP+
MDS-10
MDS-17
MDS-16
MDS-24
MDS-22
MDS-09
MDS-13
MDS-11
MDS-15
MDS-19
MDS-05
MDS-06
MDS-07
MDS-12
MDS-18
MDS-08
MDS-20
MDS-21
MDS-14
Hypermethylated genes
Hypomethylated genes
No-changed genes
B
HOXC12 (3sites)
SOX11 (11 sites)
Ave of 26 genes (115 sites)
ESPNL (3 sites)
Methylation (%)
Cord Blood
Adult Blood
MDS
AML

Figure 4

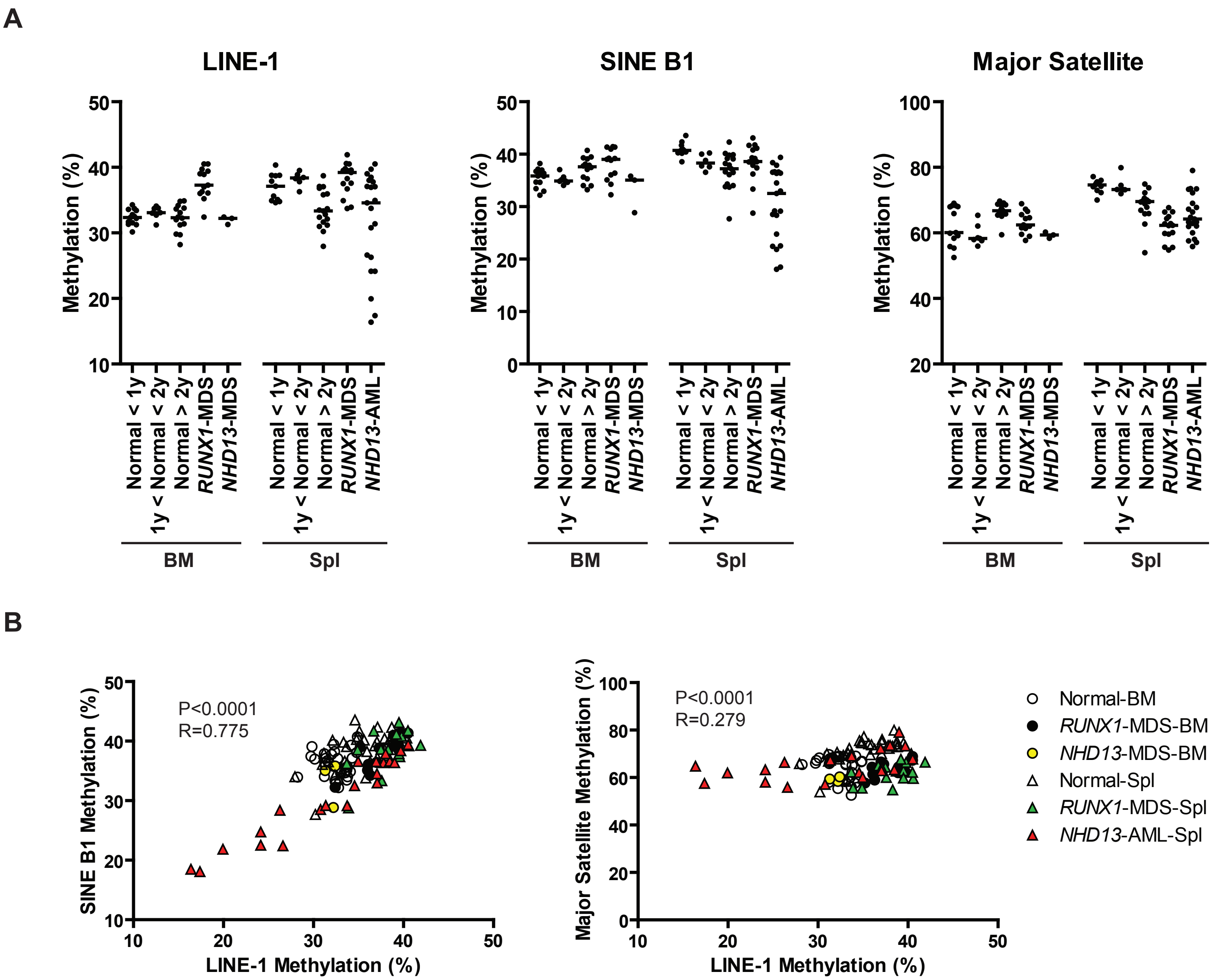
A
LINE-1
SINE B1
Major Satellite
Methylation (%)
Normal < 1y
1y < Normal < 2y
Normal > 2y
RUNX1-MDS
NHD13-MDS
NHD13-AML
BM
Spl
B
P<0.0001
R=0.775
SINE B1 Methylation (%)
LINE-1 Methylation (%)
P<0.0001
R=0.279
Major Satellite Methylation (%)
Normal-BM
RUNX1-MDS-BM
NHD13-MDS-BM
Normal-Spl
RUNX1-MDS-Spl
NHD13-AML-Spl

Figure 5